STUDIA UBB CHEMIA, LXVIII, 3, 2023 (p. 51-70)
(RECOMMENDED CITATION)
DOI:10.24193/subbchem.2023.3.04

# COMPARISON OF MEMBRANE-BASED PRE-AND POST-COMBUSTION $CO_2$ CAPTURE OPTIONS APPLIED IN ENERGY-INTENSIVE INDUSTRIAL APPLICATIONS

**Calin-Cristian CORMOS[a,*], Marius SANDRU[b], Cristian DINCA[c], Flavia-Maria ILEA[a], Alexandra DUDU[d], Mihaela Diana LAZAR[e], Nela SLAVU[c], Constantin SAVA[d], Letitia PETRESCU[a], Ana-Maria CORMOS[a], Ionela DUMBRAVA[a]**

**ABSTRACT.** Deployment of decarbonization technologies in energy-intensive industrial applications (e.g., heat and power, metallurgy, cement, chemical sectors etc.) is of great importance for reducing $CO_2$ emission and achieving global climate neutrality. Membrane $CO_2$ removal systems gained relevant attention as possible energy and cost-efficient $CO_2$ capture technology. This paper is evaluating membrane-based pre- and post-combustion $CO_2$ capture to be applied in various industrial applications with high fossil $CO_2$ emissions. The evaluation was geared mainly towards quantification of ancillary energy consumptions of membrane systems as well as the specification of captured $CO_2$ in respect to its potential utilization and storage applications. As the assessment show, the membrane-based systems are promising $CO_2$ capture technology for both pre- and post-combustion capture configurations.

***Keywords:*** *Energy-intensive industrial applications; Pre- and post-combustion $CO_2$ capture; Membrane; Ancillary energy consumptions; Technical performance indexes*

---

[a] *Babes-Bolyai University, Faculty of Chemistry and Chemical Engineering, 11 Arany Janos, RO-400028, Cluj-Napoca, Romania*

[b] *Sintef Industry, Sem Sælands vei 2 A, Trondheim, Norway*

[c] *University Politehnica of Bucharest, Faculty of Power Engineering, 313 Splaiul Independentei, RO-060042, Bucharest, Romania*

[d] *National Institute of Marine Geology and Geoecology - GeoEcoMar, 23-25 Dimitrie Onciul, RO-024053, Bucharest, Romania*

[e] *National Institute for Research and Development of Isotopic and Molecular Technologies – INCDTIM, 67-103 Donat Street, RO-400293, Cluj-Napoca, Romania*

[*] *Corresponding author: calin.cormos@ubbcluj.ro*

## INTRODUCTION

Reduction of anthropogenic $CO_2$ emissions represents a key environmental target to achieve global climate neutrality and developing the future low carbon economy. Decoupling the global energy demand from fossil $CO_2$ emissions is one of the main elements to be considered [1]. Relevant sectors of our globalized society such as industry, transport, agriculture, residential systems are due to implement efficient decarbonization strategies for both reduction of the $CO_2$ emissions and fossil energy. Several possible conceptual methods can be applied for this purpose [2] e.g., replacement of fossil energy with renewable energy sources, boosting efficiency for both conversion and utilization stages, deployment of Carbon Capture, Utilization and Storage (CCUS) systems, reduction of overall energy consumption etc. In the last years, significant political, economic, social and technological strategies were developed and planned to be deployed in practice at national and international level. For instance, the European Union (EU) aims to achieve the climate neutrality by 2050 [3].

The CCUS technologies are predicted to play a crucial role in the coming decades to achieve the climate neutrality by facilitating the transition from fossil to renewable energy sources. The $CO_2$ capture can be done is a variety of options, the most promising systems being pre- and post-combustion capture [4]. In pre-combustion capture, the gaseous fuel (e.g., syngas produced from partial oxidation technologies such as catalytic reforming or gasification) is decarbonized prior to its utilization since, in the post-combustion capture, the $CO_2$ is removed from the flue gases resulted in total oxidation (burning) processes. In respect to captured $CO_2$ destinations, it can be either geologically stored in saline aquifers, depleted oil and gas fields, unmined coal beds or used for Enhanced Oil Recovery (EOR) purposes [5]. In addition, the $CO_2$ utilization technologies by its chemical transformations to various chemicals / energy carriers (e.g., synthetic natural gas, methanol, biofuels etc.) are predicted to use the captured $CO_2$ as a valuable raw material in respect to the circular economy principles [6].

This paper assessed the membrane technology as $CO_2$ removal option in both pre- and post-combustion arrangements. As targeted industrial processes, heat and power, iron and steel, cement production plants were evaluated considering their important share in global $CO_2$ emissions. It worth mention that the non-power energy-intensive industrial processes such as steel and cement production (responsible for more than 12% global $CO_2$ emissions [7]) are hard to decarbonize due to involvement of carbon-based materials in the production scheme rather than just as fuel. For instance, in cement production, two thirds of $CO_2$ emissions are coming from the raw-materials (raw meal) decomposition and only one third from the fuel used for the thermal treatment in clincher production [8]. As targeted capacities, large scale plants were evaluated (e.g., 500-1000 MW net power, 1 Mt/y cement).

Membrane $CO_2$ capture has important features such as easy scalable technology, not requiring high energy consumptions as the chemical gas-liquid absorption [9]. All these advantages of membrane-based $CO_2$ removal systems are expected to give better techno-economic and environmental benefits. The evaluated pre- and post-combustion $CO_2$ capture systems using membrane technology were modeled and simulated using ChemCAD, the overall mass and energy balances being used for assessment of $CO_2$ capture energy penalty. In addition, the conceptual design of membrane system was chosen to satisfy the required $CO_2$ quality specification [10].

## MATHEMATICAL MODELING OF MEMBRANE $CO_2$ SEPARATION

Mathematical modeling and simulation of pre- and post-combustion $CO_2$ capture by membrane systems integrated in energy-intensive industrial processes was done by process flow modeling using ChemCAD [11]. As thermodynamic package, the Soave-Redlich-Kwong (SRK) system was chosen for the membrane $CO_2$ removal systems based on operational parameters (temperature and pressure) and present chemical species. The captured $CO_2$ is further dried for moisture removal (using an absorption – desorption cycle with Tri-Ethylene-Glycol - TEG) and compressed to 120 bar for transport to the selected utilization / storage sites.

For the post-combustion $CO_2$ capture, two distinct energy-intensive industrial cases were evaluated as follow: Case 1 - Coal-based super-critical power plant [12] and Case 2 - Conventional cement plant [13]. Figure 1 presents the conceptual layout of 3-stage membrane unit for post-combustion $CO_2$ capture to be applied in various applications (e.g., heat and power generation, metallurgy, cement, petro-chemical etc.). The 3-stage configuration was chosen taking into consideration the two combined targeted performance indicators to be simultaneously accomplished by the membrane-based $CO_2$ removal unit: 90% carbon capture rate and min. 95% (vol.) $CO_2$ concentration in the captured stream. Since the $CO_2$ concentration in the flue gases is rather low (about 12 – 15% vol. for coal-based combustion systems), a 3-stage system is required for achieving these two targets [14].

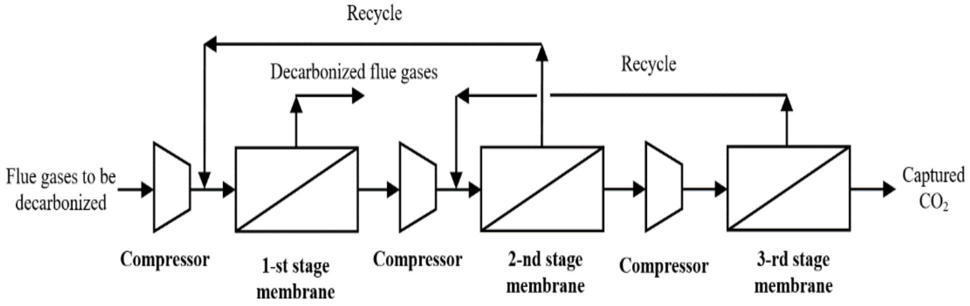

**Figure 1.** 3-stage membrane-based post-combustion $CO_2$ capture unit

For the pre-combustion $CO_2$ capture, one power generation system was evaluated as follow: Case 3 - Coal-based integrated gasification combined cycle (IGCC) power plant [15]. Figure 2 presents the conceptual layout of 2-stage membrane unit for pre-combustion $CO_2$ capture. In contrast to the post-combustion $CO_2$ capture unit which requires a 3-stage system, the pre-combustion unit requires only a 2-stage system because the $CO_2$ concentration in syngas to be decarbonize is significantly higher than for post-combustion systems (about 40% vol. for a coal-based gasification process). In addition, the pre-combustion $CO_2$ capture system uses a hydrogen selective membrane considering the differences in comparison to the post-combustion capture option [16].

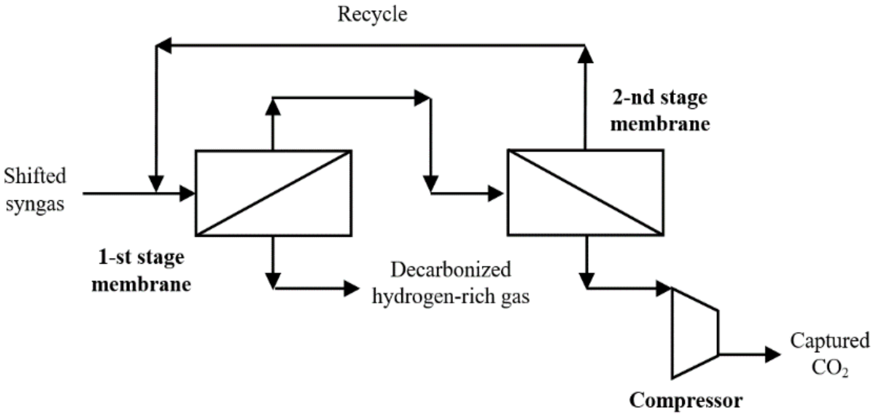

**Figure 2.** 2-stage membrane-based pre-combustion $CO_2$ capture unit

Table 1 presents the main design assumption of the investigated pre- and post-combustion $CO_2$ capture systems using membrane separation technology. In respect for the gas streams to be decarbonized (either by pre-combustion or post-combustion arrangements), the following plant capacities were used in the current analysis: Coal-based super-critical power plant (Case 1) - 1000 MW net power output [12]; Cement production plant (Case 2) - 1 Mt/y cement [17] and Coal-based Integrated Gasification Combined Cycle (IGCC) power plant (Case 3) - 450 MW net power output [18]. The evaluated pre- and post-combustion capture concepts were fully integrated in respect to mass and energy balances to give overall global performance indicators such as ancillary power consumption and cooling duties for the membrane unit and the specific primary energy consumption for $CO_2$ avoided (SPECCA) defined as follow:

- Ancillary power consumption for membrane unit was calculated as ratio of compressing work needed for flue gases and recycled gaseous streams and the mass flow of captured $CO_2$:

$$W_{Membrane\ unit} = \frac{W_{Flue\ gas\ \&\ recycle\ compression\ work}}{Captured\ CO_2\ flowrate} \tag{1}$$

- Cooling duty of membrane unit was calculated as ratio of cooling duties of the heat exchangers associated with flue gases and recycled gaseous streams and the mass flow of captured $CO_2$:

$$Cooling\ duty_{Membrane\ unit} = \frac{Q_{Flue\ gas\ \&\ recycle}}{Captured\ CO_2\ flowrate} \tag{2}$$

- Specific primary energy consumption for $CO_2$ avoided (SPECCA) was calculated for the whole decarbonized process (power plant or cement plant) as follow [19]:

$$SPECCA = \frac{3600 \cdot \left(\frac{1}{Efficiency_{CO2\ capture}} - \frac{1}{Efficiency_{No\ capture}}\right)}{CO_2\ emissions_{No\ capture} - CO_2\ emissions_{CO2\ Capture}} \tag{3}$$

**Table 1.** Main design assumptions of pre- and post-combustion $CO_2$ capture units

| **Plant sub-system** | **Design parameter** |
|---|---|
| Super-critical power plant (Case 1) flue gases | Mass flow: 1650.10 kg/s<br>Composition (vol. %): 77.11% $N_2$, 12.83% $CO_2$, 6.03% $O_2$, 3.11% $H_2O$, 0.92% Ar<br>Temperature & pressure: 50°C / 1.03 bar |
| Cement plant (Case 2) flue gases | Mass flow: 81.04 kg/s<br>Composition (vol. %): 64.80% $N_2$, 23.61% $CO_2$, 7.74% $O_2$, 3.08% $H_2O$, 0.76% Ar<br>Temperature & pressure: 40°C / 1.03 bar |
| Gasification power plant (Case 3) syngas | Mass flow: 126.28 kg/s<br>Composition (vol. %): 54.25% $H_2$, 39.84% $CO_2$, 3.25% $N_2$, 1.90% CO, 0.61% Ar, 0.15% other gases<br>Temperature & pressure: 50°C / 31 bar |
| Membrane unit - Post-combustion $CO_2$ capture (Case 1: Super-critical power plant) | $CO_2$ selective membrane<br>$CO_2$ capture rate: 90%<br>Permeance data: $CO_2$ - 370, $O_2$ - 7.41, $N_2$ - 1.85<br>Operating temperature: 50°C<br>Pressure ratio: 10<br>Compressor efficiency: 85% |
| Membrane unit - Post-combustion $CO_2$ capture (Case 2: Cement plant) | $CO_2$ selective membrane<br>$CO_2$ capture rate: 90%<br>Permeance data: $CO_2$ - 370, $O_2$ - 7.41, $N_2$ - 1.85<br>Operating temperature: 50°C<br>Pressure ratio: 10<br>Compressor efficiency: 85% |
| Membrane unit - Pre-combustion $CO_2$ capture (Case 3: Gasification plant) | $H_2$ selective membrane<br>$CO_2$ capture rate: 90%<br>Permeance data: $H_2$ - 300, $CO_2$ - 10, CO - 4, $N_2$ - 2, Ar - 2, $CH_4$ - 2, $H_2O$ - 10000<br>Pressure ratio: 5 – 10<br>Compressor efficiency: 85% |
| $CO_2$ conditioning unit (drying and compression) | Gas-liquid absorption - desorption cycle<br>Drying solvent: Tri-Ethylene-Glycol (TEG)<br>Absorber column: 4 stages<br>Desorber column: 6 stages<br>4 stages with inter-cooling compressor<br>Compressor efficiency: 85%<br>Delivery pressure: 120 bar<br>$CO_2$ composition (vol. %) [10]: >95% $CO_2$, <2000 ppm CO, <250 ppm $H_2O$, <100 ppm $H_2S$, <4% other gases ($N_2$, Ar, $H_2$) |
| Thermodynamic package | Membrane unit: Soave-Redlich-Kwong (SRK)<br>$CO_2$ drying unit: TEG Dehydration |
| Heat exchanger network | Min. temperature difference $\Delta T_{min.}$ = 10°C<br>Pressure drops: 2 – 3% from inlet pressure |

## ILLUSTRATIVE PRE- AND POST-COMBUSTION $CO_2$ CAPTURE CASES

### *1. Post-combustion decarbonization of fossil-based power plants*

The investigated coal-based super-critical power plant is generating 1000 MW net power with 90% carbon capture rate. These key design assumptions were chosen to be in line with ongoing $CO_2$ capture projects in power generation sector. As main steam cycle parameters, the following design assumptions are used: 290 bar and 582°C for the live steam with two MP steam reheats at 75 and 20 bar [20]. The conceptual design of decarbonized coal-based super-critical power plant is presented in Figure 3 and the overall key performance indicators are presented in Table 2.

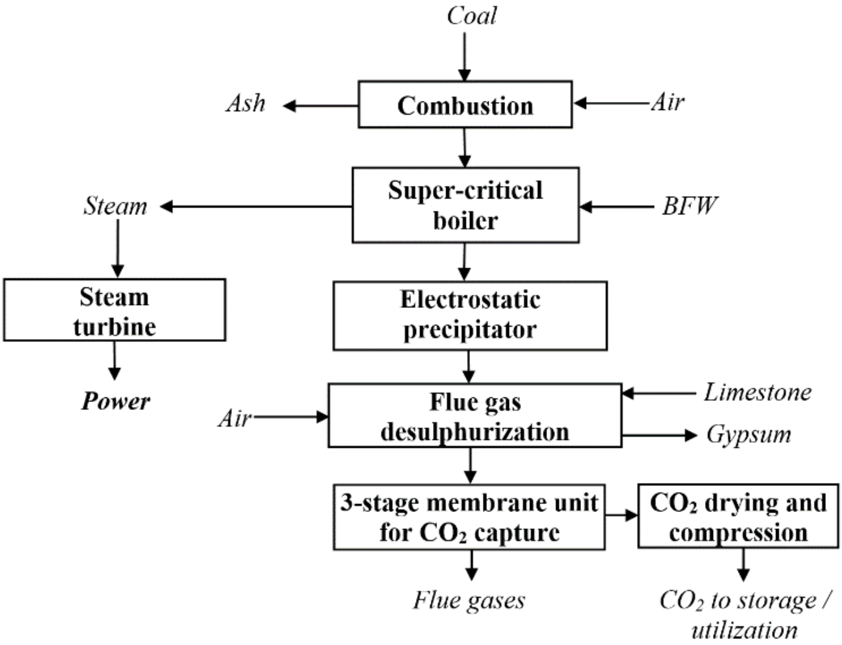

**Figure 3.** Super-critical plant with post-combustion membrane-based $CO_2$ capture

As benchmark super-critical power plant without $CO_2$ capture, a concept reported in [12] was used. One can be observed that the membrane-based $CO_2$ removal technology implies an important energy penalty for the capture (about 12 percentage points) due to the compressing large flow of flue gases. Also, the specific power consumption and cooling duty of the membrane unit are rather high as well as SPECCA indicator in comparison to the chemical scrubbing technology (3.25 vs. 2.43 GJ/t as SPECCA).

**Table 2.** Key performance indicators of decarbonized super-critical power plant

| Main performance indicator | UM | Value |
|---|---|---|
| Coal flowrate (as received basis) | t/h | 458.00 |
| Coal LHV (as received basis) | MJ/kg | 25.17 |
| Coal thermal energy – LHV (A) | $MW_{th}$ | 3202.18 |
| | | |
| Steam turbine output | $MW_e$ | 1472.75 |
| Gross power output (B) | $MW_e$ | 1472.75 |
| | | |
| Coal processing (0.5 % feedstock energy) | $MW_e$ | 16.00 |
| $CO_2$ capture & compression (membrane) | $MW_e$ | 392.35 |
| Power island consumption | $MW_e$ | 64.40 |
| Ancillary power consumption (C) | $MW_e$ | 472.75 |
| | | |
| Net power output (D = B - C) | $MW_e$ | 1000.00 |
| Gross power efficiency (B/A * 100) | % | 46.00 |
| Net power efficiency (D/A * 100) | % | 31.22 |
| Carbon capture rate | % | 90.00 |
| Specific $CO_2$ emissions | kg/MWh | 110.80 |
| SPECCA | GJ/t | 3.25 |
| | | |
| Specific power consumption membrane unit | kWh/t | 273.59 |
| Cooling duty membrane unit | GJ/t | 1.07 |

## 2. *Post-combustion decarbonization of cement plants*

The conceptual design of a decarbonized cement plant with membrane-based technology is presented in Figure 4. The overall performance indicators of the conventional cement production line as benchmark case (1 Mt/y production capacity without carbon capture) were taken from IEAGHG reports [13,21]. The additional flue gas desulphurization, membrane-based $CO_2$ capture unit and captured $CO_2$ conditioning units were simulated using ChemCAD software. The overall performance indicators of decarbonized cement plant are presented in Table 3 (the specific energy consumptions are reported on captured $CO_2$ flow while the specific $CO_2$ emission is reported on cement output).

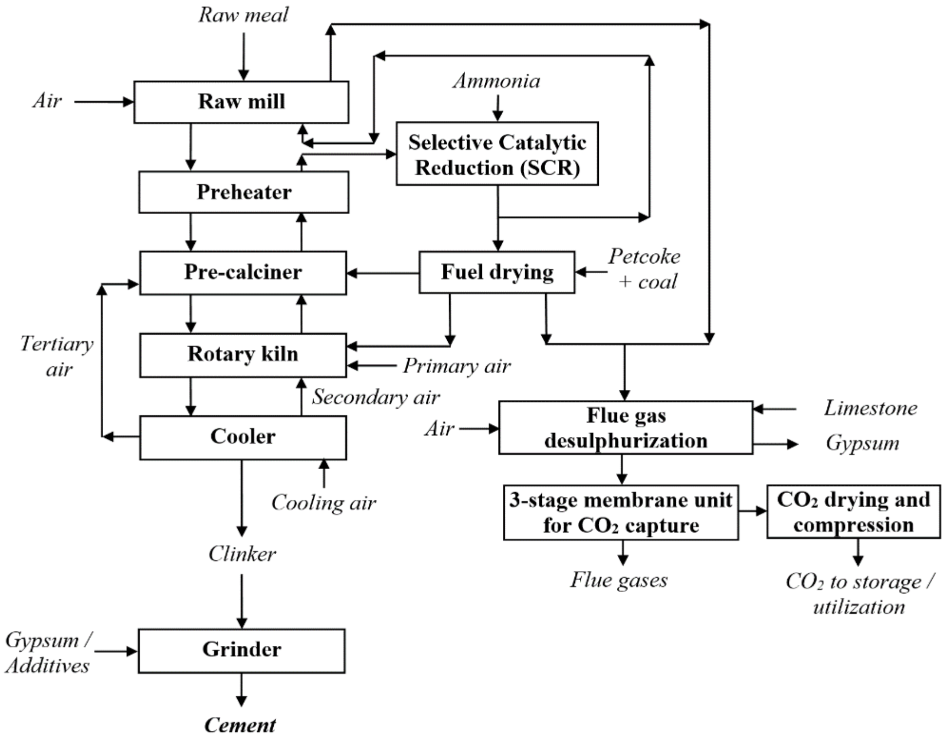

**Figure 4.** Cement plant with post-combustion membrane-based $CO_2$ capture

**Table 3.** Key performance indicators of decarbonized cement plant

| Main performance indicator | UM | Value |
|---|---|---|
| Cement plant capacity | kt/y | 1000 |
| Coal and petcoke flowrate (cement line) | t/h | 12.20 |
| | | |
| $CO_2$ capture & compression (membrane unit) | $MW_e$ | 31.20 |
| Power consumption (cement line) | $MW_e$ | 10.20 |
| Ancillary power consumption (whole plant) | $MW_e$ | 41.40 |
| | | |
| Carbon capture rate | % | 90.00 |
| Specific $CO_2$ emissions (incl. power import) | kg/t | 233.60 |
| SPECCA | GJ/t | 2.65 |
| | | |
| Specific power consumption membrane unit | kWh/t | 206.82 |
| Cooling duty membrane unit | GJ/t | 0.64 |

It can be observed that in comparison to super-critical power plant, the ancillary energy consumptions (both power and cooling duties) of the membrane unit is lowered for the cement plant. This can be explained by the fact that a lower flow of more $CO_2$ concentrated flue gases is to be treated for decarbonisation. Also, the SPECCA indicator is significantly reduced in comparison to chemical gas-liquid absorption (2.65 vs. 5.4 GJ/t).

### *3. Pre-combustion decarbonization of partial oxidation plants*

The conceptual design of a decarbonized coal-based IGCC power plant with membrane-based technology is presented in Figure 5 [22].

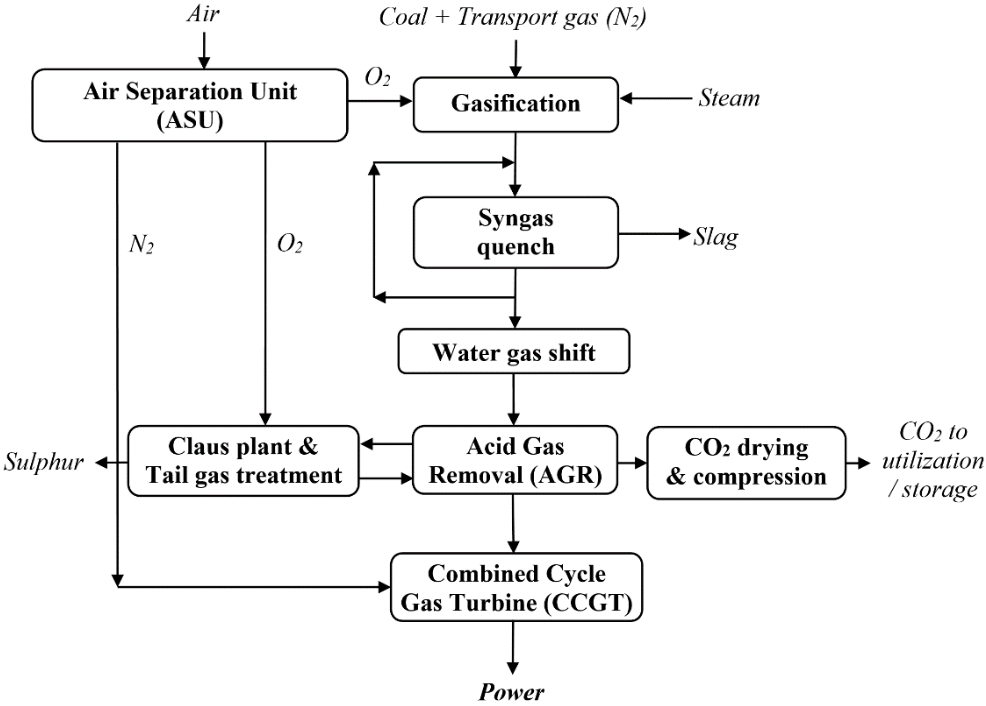

**Figure 5.** IGCC power plant with pre-combustion membrane-based $CO_2$ capture

The evaluated IGCC power plant was based on Shell gasification technology [23] and Mitsubishi gas turbine combine cycle unit [24]. Table 4 presents the overall performance indicators of decarbonized IGCC power plant using pre-combustion membrane-based $CO_2$ capture.

**Table 4.** Key performance indicators of decarbonized IGCC power plant

| Main performance indicator | UM | Value |
|---|---|---|
| Coal flowrate (as received basis) | t/h | 168.50 |
| Coal LHV (as received basis) | MJ/kg | 25.17 |
| Coal thermal energy – LHV (A) | $MW_{th}$ | 1178.09 |
| | | |
| Gas turbine output | $MW_e$ | 334.00 |
| Steam turbine output | $MW_e$ | 217.25 |
| Gross power output (B) | $MW_e$ | 552.25 |
| | | |
| Air separation unit consumption | $MW_e$ | 43.12 |
| Gasification island consumption | $MW_e$ | 10.00 |
| $CO_2$ capture & compression (membrane) | $MW_e$ | 30.75 |
| Power island power consumption | $MW_e$ | 19.80 |
| Ancillary power consumption (C) | $MW_e$ | 103.67 |
| | | |
| Net power output (D = B - C) | $MW_e$ | 448.58 |
| Gross power efficiency (B/A * 100) | % | 46.87 |
| Net power efficiency (D/A * 100) | % | 38.07 |
| Carbon capture rate | % | 90.00 |
| Specific $CO_2$ emissions | kg/MWh | 91.50 |
| SPECCA | GJ/t | 2.46 |
| | | |
| Specific power consumption membrane unit | kWh/t | 51.40 |
| Cooling duty membrane unit | GJ/t | 0.11 |

As can be noticed, the membrane-based pre-combustion $CO_2$ capture technology has lower ancillary energy consumption than the corresponded post-combustion capture options (due to high $CO_2$ partial pressure in the gas to be treated for decarbonization). For instance, the specific power consumption and cooling duty for the membrane $CO_2$ removal unit are significantly reduced by about 75 - 80%, respectively by about 83 - 90%. Also, the SPECCA indicator is lower for gasification-based power plants than for combustion-based power plants (2.46 vs. 3.25 GJ/t). As key conclusion from the evaluation is that the membrane-based decarbonization technology is more suitable for pre-combustion capture (applied in gasification and reforming processes) than for the post-combustion capture.

## CAPTURED $CO_2$ PROPERTIES AND ITS UTILISATION & STORAGE

The quality specifications of the captured $CO_2$ streams from the three investigated decarbonized plant concepts using membrane-based pre- and post-combustion configurations in respect to the accepted literature specification [10] are presented in Table 5 together with their main characteristics (mass flows, pressure and temperature).

**Table 5.** Captured $CO_2$ streams characteristics

| Parameter | Literature | Case 1 | Case 2 | Case 3 |
|---|---|---|---|---|
| Mass flowrate (t/h) | NA | 1031.38 | 83.13 | 374.38 |
| Pressure (bar) | NA | 120 | 120 | 120 |
| Temperature (°C) | NA | 40 | 40 | 40 |
| Composition (vol. %) | | | | |
| $CO_2$ | Min. 95.00 | 96.34 | 97.10 | 98.02 |
| CO (ppm) | Max. 2000 | 800 | 500 | 600 |
| Water (ppm) | Max. 500 | 100 | 150 | 100 |
| Sulphur species (ppm) | Max. 200 | 50 | 50 | 50 |
| Other non-condensable components ($N_2$, Ar, $H_2$) | Max. 4.00 | 3.56 | 2.83 | 1.90 |

As can be noticed for all investigated cases, the quality specifications of the captured $CO_2$ are fully in line with literature references. After capture and conditioning, the captured $CO_2$ can be used for transformation into various chemicals / energy carriers (e.g., synthetic natural gas, methanol, synthetic fuels) or geologically stored (e.g., saline aquifers, depleted hydrocarbon fields or used for Enhanced Oil Recovery - EOR).

For instance, in term of $CO_2$ utilization possibilities, its transformation in value added products by catalytically hydrogenation is the most promising and straightforward option. In this regard several directions are investigated: (i) syngas production either by reverse water gas shift, by dry reforming or by combined steam and dry reforming; (ii) production of synthetic fuels such as methane, methanol etc. (iii) $CO_2$ involvement in chemical hydrogen storage cycles as $CO_2 + H_2 \leftrightarrow HCOOH$; (iv) $CO_2$ transformation in chemicals: ethylene, monomers/polymers, urea, fine chemicals etc.

From all these possibilities, the $CO_2$ methanation process (Sabatier process, see reaction 4) is the most studied due to its part in the Power-to-methane concepts to enhance renewable power utilization [25].

$$CO_2 + 4H_2 \leftrightarrow CH_4 + 2H_2O \qquad \Delta H = -165 \text{ kJ/mol (298K)} \qquad (4)$$

In this concept, the extra power obtained from renewable sources (e.g., solar and wind applications) at peak generation is chemically stored as synthetic methane, mitigating thus one of the most important problems of renewable power, which is its time unpredictable generation.

Although favorized from thermodynamically point of view, the reaction 4 is kinetically limited, as 8 electrons are needed in the reduction process of carbon dioxide. The main problem is the high stability of the $CO_2$ molecule making its chemical transformation highly unfavorable. In these conditions, the presence of an active catalyst is mandatory for the process to become energy- and cost-efficient [26]. Also, the selectivity of catalyst for methane formation is of main importance for overall process performance, as many other products can be formed from hydrogen and carbon dioxide.

The composition of captured $CO_2$, as presented in Table 8, is proper for its direct use in the $CO_2$ methanation reaction without other modifications. The reaction mixture tested in this work consists in $CO_2$, $H_2$ and Ar in molar ratio $CO_2 / H_2 / Ar = 1 / 4.5 / 1$. In these testing conditions, the sulphur species which can negatively intervene in catalyst activity and stability are in very low concentrations (at the ppm level due to previous cleaning). Water or CO are also in low proportion and the non-condensable gases does not interfere in the catalytic process. Using Ni as active metal and a combination of oxides as support, the $CO_2$ can be transformed in synthetic methane with good conversion and selectivity in relatively mild conditions. The best results were obtained using Ni(14wt.%)/$La_2O_3$(10wt.%)-$SiO_2$ catalyst for which a 72% $CO_2$ conversion rate and a total methane selectivity were obtained at 350°C, atmospheric pressure and 5500 $h^{-1}$ Gas Hourly Space Velocity (GHSV) as experimental testing conditions.

The Combined Steam and Dry Reforming of Methane (CSDRM) represents the parallel and concomitant reformation reaction of methane with $H_2O$ and $CO_2$ (see reactions 5 and 6) [27].

$$CH_4 + CO_2 \leftrightarrow 2CO + 2H_2 \qquad (5)$$

$$CH_4 + H_2O \leftrightarrow CO + 3H_2 \qquad (6)$$

As a way for $CO_2$ valorization, the CSDRM presents a series of advantages compared to both individually, dry reforming (reaction 5) and steam reforming (reaction 6) such as: (i) the composition of synthesis gas can be designed by adjusting the ratio of water in the mixture; it is thus possible to design the experimental conditions which provide directly syngas with proper composition for the Fischer-Tropsch process for superior hydrocarbon synthesis ($H_2$ : CO molar ratio of 2 : 1); (ii) the catalysts' stability and lifetime are significantly improved compared to the dry reforming process due to less carbon formation.

Among the best catalysts for this reaction are Ni-based ones. When Ni is supported on alumina doped with basic or reducible oxides very good results are obtained at medium temperatures, as demonstrated by our group previous studies [28-29]. The Ni/$La_2O_3$-$Al_2O_3$ catalyst possess a very capacity to disperse and stabilize the Ni nanoparticles on the support, increasing thus significantly both the catalytic activity and catalyst stability against deactivation. Regarding the Ni/$CeO_2$-$Al_2O_3$ catalyst, the redox and oxygen storage properties of ceria positively intervene in the reaction mechanism, improving substantially the catalytic performances. In all mentioned cases, the produced synthesis gas is of good quality with $H_2$ : $CO_2$ molar ratio of 2.3 - 2.5 is obtained.

Both presented $CO_2$ utilization routes by catalytic processes, described above (methanation and CSDRM concepts) present real opportunities for up-scaling and large-scale deployment. In this respect, some pilot plants being already in function [25]. By developing new catalysts as those described above, the economic efficiency of the $CO_2$ hydrogenation processes can be improved, making the $CO_2$ utilization a viable option and contributing thus to the attractivity of general CCUS technologies.

In respect to the $CO_2$ transport and storage options, several targeted onshore geological locations within Romania (e.g., Oltenia and Galati regions) were considered within this study. As transport options, road truck / rail tanks and pipeline are the most promising technical options with a distinct advantage for the pipeline transport considering the high volumes of $CO_2$ to be transported (see Table 5). The $CO_2$ transportation costs can have a significant impact on the overall economics of a $CO_2$ storage project [30]. Therefore, it is important to carefully consider the transport parameter when selecting a suitable site for $CO_2$ storage and / or used for Enhanced Oil Recovery (EOR). This involves analyzing the transport distance between the source of $CO_2$ (e.g., energy-intensive industrial processes such as power plants, cement and steel mills) and the potential storage sites, as well as the available means of transport and their associated economic costs. By carefully considering these factors, the most cost-effective and feasible transport option for a given $CO_2$ storage project is chosen. As $CO_2$ transport costs, most of under-development large-scale CCUS projects consider an average value of 10 €/t [31].

In respect to the $CO_2$ geological storage, two onshore potential sites were evaluated by project partner GeoEcomar as follow: the Oltenia region is which both saline aquifers and depleted oil and gas reservoirs were identified and characterized in term of storage capacity and the Galati region is which both onshore and offshore storage were identified (using depleted oil and gas fields as well as EOR). As the $CO_2$ storage costs, most of under-development large-scale CCUS projects consider an average value of 10-15 €/t [32]. In respect to the $CO_2$ storage capacities, the Oltenia region has a capacity of about 1.5 million tons per year in onshore deep saline aquifers in a radius of 50 km from the power plant as evaluated in the CCS Getica demo project which evaluated the potential decarbonization of Turceni power plant [33]. It worth also mention that the large-scale deployment of any decarbonization technologies implies a significant increase of power / cement production costs (starting from at least 30 - 50% [17,24,34]).

## CONCLUSIONS

This paper presents the main experimental and numerical investigation devoted to the integration of membrane technology as pre- and post-combustion decarbonization option for various energy-intensive industrial applications (e.g., heat and power generation, cement etc.). Also, relevant aspects are evaluated in respect to the captured $CO_2$ utilization (for catalytic transformation to various energy carriers / chemicals) and geological storage. As key result of the experimental and numerical investigations, one can noticed the promising performances of membrane-based decarbonization technology applied to pre-combustion capture systems in comparison to the post-combustion capture systems e.g.: lower specific power consumption for the membrane unit (52 kWh/t vs. 206 - 274 kWh/t), lower specific primary energy consumption for $CO_2$ avoided (2.46 GJ/t vs. 3.25 GJ/t), lower cooling duty of the membrane unit (0.1 GJ/t vs. 0.64 - 1.1 GJ/t). The investigated membrane-based decarbonization systems (either pre-combustion or post-combustion cases) delivered the captured $CO_2$ stream within the quality specification considered for various $CO_2$ utilization (e.g., methanation process) and storage applications (e.g., saline aquifers or utilization for EOR purposes).

## EXPERIMENTAL

### *Membrane-based $CO_2$ separation*

The experimental analysis consisted of testing the durability of the membranes. The membranes were exposed to flue gases from the lignite combustion of the Circulating Fluidized Bed Combustion (CFBC) pilot plant at the University Politehnica of Bucharest, Power Engineering Faculty. The membranes analyzed were developed and produced by SINTEF, Trondheim, Norway. The following membranes were tested for durability:

Flat sheet membranes:

- Poly-dimethyl-siloxane on poly-acrylonitrile (PDMS/PAN);
- PSF coated with polyacrylamide (PAA/PSF);
- Mixed matrix membrane (RTI);

Hollow fibers membranes:

- Poly-p-phenylene oxide (PPO);
- Poly-sulfone (PSF).

Figure 6 shows the CFBC installation with pilot unit for assessing the durability membrane testing in real plant operating conditions. The evaluated membranes (up to 6 samples in the same time) are positioned on the sampler on the vessel bottom. The flue gases from CFBC unit are extracted with a compressor but because the flue gases temperature is higher than the temperature required by compressor a heat exchanger (air-flue gases) need to reduce the temperature around 80°C.

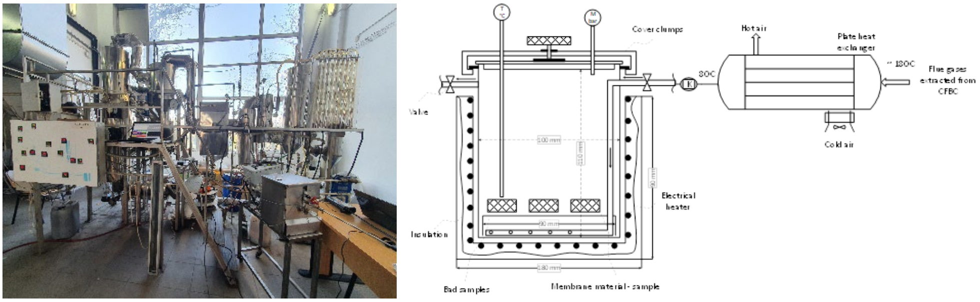

**Figure 6.** CFBC with pilot membrane testing installation (left). Schematic diagram of the pilot membrane testing installation (right)

For beginning of membrane unit operation, the inlet and outlet valves are opened, and the flue gases enter the reactor, eliminating the air from the enclosure. This process takes several minutes. Further, the left valve is closed so that the flue gases introduced fill the entire volume of the reactor. The evaluated membranes are put on the bed provided inside the testing enclosure. After this step, the potentiometer of the electrical resistance is set at the desired testing temperature. When the desired pressure has been created, the right valve is closed. The evaluated membranes were exposed to flue gas with the composition shown in Table 6 for about 504 hours at a temperature between 50-60°C and atmospheric pressure. These testing conditions are similar to industrial processes such as CFBC power plants.

**Table 6.** Flue gas composition used for membrane testing

| $O_2$ % | $CO_2$ % | NO ppm | $NO_x$ ppm | $SO_2$ ppm | $T_{gas}$°C | λ |
|---|---|---|---|---|---|---|
| 6.52 | 12.67 | 176 | 185 | 570 | 51.50 | 1.43 |

The evaluated membranes were characterized using the Fourier-transform infrared spectroscopy (FTIR) spectroscopy, water contact angle, scanning electron image and gas permeation properties before and after flue gas exposure at a specific temperature (similar to real power plant operation). From the appearance of membranes after flue gas exposure, it can be noted a small coloring (yellowish) and as well the presence of dust/carbon particles from flue gas (see Figure 7). No major changes in membrane structure were observed during the testing procedure.

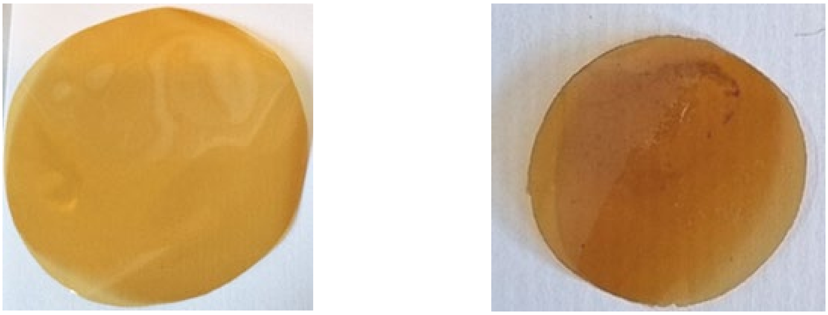

**Figure 7.** Images of tested membrane before (left) and after (right) the flue gas exposure for RTI case

The contact angle using water was performed in order to assess the deposition of dust / carbon or a change in membrane surface chemistry (e.g. oxidation) during its practical operation in a $CO_2$ capture process.

**Table 7.** Contact angle results before and after flue gas exposure

| **Polymer membrane** | **Contact angle** | |
|---|---|---|
| | Before | After |
| PDMS-PAN | 99.00 | 96.80 |
| Polyacrylamide | 70.00 | 64.00 |

The contact angle results presented in Table 2 show a small decrease indicating that exposure of membranes to flue gas hydrophilized the surface or some solid material was deposited on the surface. The changes are small and do not indicate a considerable change that needs to be addressed by membrane optimization. The membranes were tested using a gas mixture of synthetic flue gas 10% $CO_2$ in $N_2$ at a pressure of 1.2 bar, at 25ºC and 100% relative humidity. The key results of the membrane gas permeation are presented in Table 8 for some illustrative cases.

**Table 8.** Summary of gas permeation before and after flue gas exposure

| **Type of membrane** | **$CO_2$ Permeance [$m^3$(STP)/($m^2$ bar h)]** | | **$CO_2$/$N_2$ Selectivity** | |
|---|---|---|---|---|
| | Before | After | Before | After |
| Flat sheet membranes | | | | |
| Mixed matrix membrane (RTI) | 0.0029 | 0.0022 | 48.00 | 31.00 |
| PDMS/PAN | 1.20 | 0.23 | 11.00 | 12.00 |

After the experimental analysis for their durability, some changes were observed to the tested membranes. If for the RTI membranes, the $CO_2$ permeance remain practically unchanged before and after flue gas exposure, an about 35% decrease of selectivity was observed. For the PDMS/PAN membrane, the selectivity remained unchanged but the permeance decreased after exposure. For the PDMS/PAN membranes, the gas permeation reduction of the $CO_2$ permeance, indicated perhaps the deposition of an extra layer-this need to be investigated by FT-IR, EDX, etc.

## ACKNOWLEDGMENTS

This work was supported by the NO Grants 2014 - 2021, under project contract no. 13/2020.

## REFERENCES

1. Y. Wu; Q. Zhu; B. Zhu; *Energy Policy*, **2018**, *116*, 30-38
2. D. V. Quang; D. Milani; M. Abu Zahra; *Int. J. Greenh. Gas Control*, **2023**, *124*, 103862
3. European Commission, The European Green Deal, COM(2019) 640 final, Brussels, Belgium, **2019**
4. J. A. Garcia; M. Villen-Guzman; J. M. Rodriguez-Maroto; J. M. Paz-Garcia; *J. Environ. Chem. Eng.*, **2022**, *10*, 108470
5. M. Ali; N. K. Jha; N. Pal; A. Keshavarz; H. Hoteit; M. Sarmadivaleh; *Earth-Sci. Rev.*, **2022**, *225*, 103895
6. K. Zhi; Z. Li; B. Wang; J. J. Klemeš; L. Guo; *Process Saf. Environ. Prot.*, **2023**, *172*, 681-699

7. C. da Silveira Cachola; M. Ciotta; A. Azevedo dos Santos; D. Peyerl; *Carbon Capture Sci. Technol.*, **2023**, *7*, 100102
8. E. Benhelal; E. Shamsaei; M. I. Rashid; *J. Environ. Sci.*, **2021**, *104*, 84-101
9. P. Luis; T. van Gerven; B. van der Bruggen; *Prog. Energ. Combust.*, **2021**, *38*, 419-448
10. E. de Visser; C. Hendriks; M. Barrio, M. J. Mølnvik; G. Koeijer; S. Liljemark; Y. L. Gallo; *Int. J. Greenh. Gas Control*, **2008**, *2*, 478-84
11. Chemstations, ChemCAD - Chemical Process Simulation, http://www.chemstations.net/; 2023
12. C. C. Cormos; C. Dinca; *Energy*, **2021**, *220*, 119734
13. International Energy Agency - Greenhouse Gas R&D Programme (IEAGHG), $CO_2$ capture in the cement industry, Report 2008/3, Cheltenham, UK, 2008
14. H. Wu; Q. Li; M. Sheng; Z. Wang; S. Zhao; J. Wang; S. Mao; D. Wang; B. Guo; N. Ye; G. Kang; M. Li; Y. Cao; *J. Membr. Sci.*, **2021**, *624*, 119137
15. A. M. Cormos; S. Dragan; C. C. Cormos; *Appl. Therm. Eng.*, **2022**, *205*, 118078
16. L. Giordano; J. Gubis; G. Bierman; F. Kapteijn; *J. Membr. Sci.*, **2019**, *575*, 229-541
17. C. C. Cormos; *Fuel*, **2022**, 320, 123907
18. International Energy Agency - Greenhouse Gas R&D Programme (IEAGHG), Potential for improvement in gasification combined cycle power generation with $CO_2$ capture, Report PH4/19, Cheltenham, UK, 2003
19. G. Manzolini; A. Giuffrida; P. D. Cobden; H. A. J. van Dijk; F. Ruggeri; F. Consonni; Int. J. Greenh. Gas Control, **2020**, *94*, 102935
20. A. M. Cormos; C. C. Cormos; *Appl. Therm. Eng.*, **2017**, *127*, 106-115
21. International Energy Agency - Greenhouse Gas R&D Programme (IEAGHG), Deployment of CCS in the cement industry, Report 2013/19, Cheltenham, UK, 2008
22. U.S. Department of Energy - National Energy Technology Laboratory (NETL), Cost and performance baseline for fossil energy plants. Volume 1a: Bituminous coal (PC) and natural gas to electricity, Report DOE/NETL-2015/1723, USA, 2015
23. C. Higman; M. van der Burgt; *Gasification*, 2nd ed.; Oxford: Elsevier Science, Gulf Professional Publishing, 2008
24. C. C. Cormos; *Energy*, **2012**, *42*, 434-445
25. M. D. Lazar; M. Mihet; M. Dan; Hydrogen to Methane-An Important Step in the Power-to-Gas Concept. In: *Comprehensive Renewable Energy*, M. Letcher Trevor Eds.; 2nd edition, **2022**, vol. 4, pp. 553–565. Oxford: Elsevier. http://dx.doi.org/10.1016/B978-0-12-819727-1.00032-7
26. G. Torres-Sempere; L. Pastor-Perez; J. A. Odriozola; J. Yu; F. J. Duran-Olivencia; L. F. Bobadilla; T. R. Reina, *Curr. Opin. Green Sustain. Chem*. **2022**, *36*, 100647
27. A. S. Farooqi; M. Yusuf; N. A. Mohd Zabidi; R. Saidur; K. Sanaullah; A. S. Farooqi; A. Khan; B. Abdullah, *Int. J. Hydrog. Energy*, **2021**, *46*, 31024-31040
28. M. Dan, M. Mihet, G. Borodi, M. D. Lazar, *Catal. Today*, **2021**, *366*, 87-96
29. M. Dan, M. Mihet, L. Barbu-Tudoran, M. D. Lazar, *Microporous Mesoporous Mater.,* **2022,** *341*, 112082

30. E. Smith; J. Morris; H. Kheshgi; G. Teletzke; H. Herzog; S. Paltsev; *Int. J. Greenh. Gas Control*, **2021**, *109*, 103367
31. S. Roussanaly; G. Bureau-Cauchois; J. Husebye; *Int. J. Greenh. Gas Control*, **2013**, 12, 341-350
32. C. C. Cormos, *Energy*, **2023**, *170,* 126926
33. Global CCS Institute, Getica CCS project, Public report, https://www.globalccsinstitute.com/archive/hub/publications/25516/getica-251111v2.pdf, 2011
34. K. Storrs; I. Lyhne; R. Drustrup; *Int. J. Greenh. Gas Control*, **2023**, *125*, 103878